Earth System Dynamics
Discussions
Open Access
EGU

Consistent increase of East Asian Summer Monsoon rainfall and its variability under climate change over China in 34 coupled climate models

Anja Katzenberger[1,2] and Anders Levermann[1,2,3]

[1]Potsdam Institute for Climate Impact Research, Potsdam, Germany
[2]Potsdam University, Potsdam, Germany
[3]LDEO, Columbia University, New York, USA

Correspondence: Anja Katzenberger (anja.katzenberger@pik-potsdam.de)

1 **Abstract.** The East Asia Monsoon (EAM) dominates the climate over the densely populated East China and adjacent regions
2 and is therefore influencing a fifth of the world's population. Thus, it is highly relevant to assess the changes of the central
3 characteristics of the East Asian Summer Monsoon (EASM) under future warming in the latest generation of coupled climate
4 models of the Coupled Model Intercomparison Project Phase 6 (CMIP6). Using 34 CMIP6 models we show that all models
5 that capture the EASM in the reference period 1995-2014 within two standard deviations project an increase in June-August
6 rainfall independent of the underlying emission scenario. The multi-model mean increase is 17.2% under SSP5-8.5, 12.7%
7 under SSP3-7.0, 11.9% under SSP2-4.5 and 11.2% under SSP1-2.6 in the period 2081-2100 compared to 1995-2014. For
8 China, the projected monsoon increase is slightly higher (12.1% under SSP1-2.6 and 19.1% under SSP5-8.5). The EASM
9 rainfall will particularly intensify in South-East China, Taiwan as well as North Korea. The multi-model mean indicates a
10 linear relationship of the EASM rainfall depending on the global mean temperature relatively independent of the underlying
11 scenario: Per degree of global warming, the rainfall is projected to increase by 0.14mm/day which refers to 3% of rainfall in
12 the reference period. It is thus predominately showing a "wet-region-get-wetter" pattern. The interannual variability is also
13 robustly projected to increase between 7.0% under SSP1-2.6 and 31.4% under SSP5-8.5 in the multi-model mean between
14 2050-2100 and 1965-2015. Comparing the same periods, extremely wet seasons are projected to occur 6.5-times more often
15 under SSP5-8.5.

16 **Keywords:** East Asian Monsoon, Monsoon, CMIP6, climate models, China

1 Introduction

18 The climate over East Asia is dominated by the monsoon seasons which are defined as reversing seasonal winds between the
19 Pacific Ocean and the East Asian continent associated with different rainfall regimes. Rainfall during the East Asian Summer
20 Monsoon (EASM) accounts for 40–50% of the annual precipitation in South China and 60–70% of the annual precipitation in
21 North China (Lei et al., 2011) making it a central factor for the socioeconomic livelihoods in the region.

During mid may, rainfall surges over the South China Sea establishing a planetary-scale monsoon rainband extending from the South Asian marginal seas to subtropical western North Pacific. The monsoon then gradually progresses towards inland resulting in the synchronized onset of the Indian monsoon season as well as the the monsoon season in China and Japan in early June (Wang et al., 2002). During the summer months, low level southerly winds transport moisture to East China, Korea and Japan where it converges within the rain belt that is called the Meiyu in China, the Baiu in Japan, and the Changma in Korea. The wind direction follows the pressure gradient resulting from a zonal land-sea thermal contrast varying throughout the course of a year (Ha et al., 2012; Wang et al., 2002). The rainfall reaches its maximum in late June over the Meiyu/Baiu and in late July over northern China. Then, the rainy season retreats progressively poleward in East Asia during July and August, while southward in the Indian summer monsoon (Wang et al., 2002).

Since the East Asian Monsoon is located in the subtropics - unlike other monsoon systems, it is additionally influenced by mid-latitude disturbances and convective activity (Ha et al., 2012). Besides, the EAM interacts with various climatological patterns on various time scales, including El Niño-Southern Oscillation (ENSO), the Arctic Oscillation (AO), the Indian summer monsoon, spring Eurasian snow cover and the thermal forcing of the Tibetan Plateau (Ha et al., 2012).

The progressing and retreat of the Meiyu belt is associated with a large variability of precipitation over East Asia and accompanied by floods and droughts with potentially devastating impacts on socioeconomic livelihood (Yihui et al., 2020). In June and July 2020 large parts of East and South Asia were flooded as a result of excessive monsoon rainfall affecting approx. 35 mio. individuals (Volonté et al., 2021). Therefore, assessing the climate model projections of the East Asian summer monsoon under climate change is of critical importance for national and regional management strategies.

The central approach to assess changes in the East Asian monsoon throughout the 21st century are global climate models. The general circulation models (GCM) participating in the Coupled Model Intercomparison Project (CMIP) have provided some insight regarding future changes of the EAM. The models from the previous generation (CMIP5) project an increase of the East Asian Monsoon of 10–15% throughout the 21st century under RCP6.0, most pronounced over the Baiu region and over the north and northeast of the Korean Peninsula (Seo et al., 2013). The strengthening of monsoon rainfall is attributed to an increase in evaporation as well as moist flux convergence induced by the (north) westward shift of the North Pacific subtropical high (Lee and Wang, 2014; Seo et al., 2013). Besides, the CO_2-induced strengthening of the land-sea thermal contrast plays a central role for the Asian monsoon (Endo et al., 2018). Chen and Sun (2013) find that the frequency and intensity of intense precipitation events are also projected to significantly increase over East Asia under RCP4.5.

The continuous development of the GCMs in CMIP has also lead to the improvement of the models' performance regarding the East Asian Monsoon. While most CMIP3 models show a limited capacity in simulating the precipitation over East Asian monsoon areas (Kai et al., 2009; Chen and Sun, 2013), the previous generation models of CMIP5 provided improvements regarding observed spatial and temporal precipitation patterns (Seo et al., 2013). Nevertheless, CMIP5 models struggle to reproduce rainfall bands around 30°N as well as the northward shift of the western North Pacific subtropical high (Huang et al., 2013).

Further progress has been made by CMIP6 models that outperform their predecessors regarding the EAM in past periods (Jiang et al., 2020; Xin et al., 2020; Yu et al., 2023). These improvements are related to the reduced biases in the sea surface

57 temperature (SST) over the Northwestern Pacific Ocean and better spatial resolution (Xin et al., 2020). In general, the CMIP6

58 models have reliable abilities in capturing the main characteristics of the East Asian monsoon, including the spatial distribution

59 of temperature and precipitation over China and the interannual variation (Xin et al., 2020; Masson-Delmotte et al., 2021).

60 However GCMs simulate 16-80% more national rainfall compared to observations during 1979-2005 (Jiang et al., 2020).

61   Previous studies have compared CMIP5 and CMIP6 models for past periods (Jiang et al., 2020; Xin et al., 2020; Yu et al.,

62 2023) or evaluated the changes of EASM in observations and CMIP6 models for 1979-2010 (Park et al., 2020) or analysed

63 the inter-model spread for 1979-2014 (Huang et al., 2022). Other studies have analysed the CMIP6 projections for the EAM

64 but only in the context of the global monsoon (Moon and Ha, 2020; Chen et al., 2020; Wang et al., 2020) and Asia monsoon

65 (Ha et al., 2020) neglecting e.g. regional model performance. To the best of the authors' knowledge, no study has put the

66 focus on the EAM providing detailed insight into projections for the EASM seasonal mean, its interannual variability as

67 well as the occurrence of extremely wet seasons for different time periods in the future under different emission scenarios.

68 Besides, we provide the central projections for China specifically, as highly relevant to policy makers. Here, we use the latest

69 generation of climate models in order to update the projected changes of the EAM rainfall under different socioeconomic

70 scenarios throughout the 21st century. For this purpose, we compare the available models and choose the ones with the best

71 performance for the further analysis. Section 2 provides a brief overview of the underlying climate model data and the Methods.

72 In Subsection 3.1, we divide the available models according to their performance in modeling the EASM in an historic period

73 in two groups. Subsection 3.2 presents the results of the mean summer monsoon precipitation, while Subsection 3.3 focuses on

74 the long-term trend of interannual variability and Subsection 3.4 provides further insights regarding the frequency of extremely

75 wet seasons. The results are discussed and concluded in Section 4.

2 Methods

77 In this study, we use 34 CMIP6 models that were available for the historic period (1850-2014) as well as for the future period

78 (2015-2100) under SSP5-8.5 in ScenarioMIP (O'Neill et al., 2016; Tebaldi et al., 2020). Per model center, a maximum of two

79 model configurations is used in order not to create bias. We use four scenarios (SSP1-2.6, SSP2-4.5, SSP3-7.0, SSP5-8.5) that

80 are based on different socioeconomic pathways with their associated greenhouse gas emissions as well as aerosol pollution

81 levels. These pathways are then translated into the resulting forcing levels (Van Vuuren et al., 2014; O'Neill et al., 2017). Table

82 1 provides an overview of the availability of the models in the different scenarios. The resolution of the native grids in which

83 the simulations were run are presented in Table A1 ranging from 2.5 to 500km. For the analysis, we regrid the model grids

84 to uniform 1°longitude x 1°latitude grids by first order conservative remapping. We use one ensemble member per model (if

85 available r1i1p1f1). Following existing literature, we focus on the land area in 20-50°N and 100-150°E to cover the East Asian

86 Monsoon (See Fig. A1). We obtain mean rainfall by averaging the monthly rainfall data during the summer monsoon season

87 from June to August. We use the future period from 2081-2100 and compare it to the reference period 1995-2014 in accordance

88 with the IPCC guidelines (Masson-Delmotte et al., 2021). For the analysis of the interannual variability and the occurrence of

89 extremely wet seasons, we compare 2050-2100 to 1965-2015 in order to have longer time periods and robuster results. For the

Earth System
Dynamics
Discussions

Table 1. Overview of data availability for the 34 models used in the study (precipitation/temperature). Only those models are selected for which data for historic period and SSP5-8.5 was available at the time of the study. Y indicates availability, N marks models that were not available for the scenario.

Modeling Center (Group)	Model	SSP1-2.6	SSP2-4.5	SSP3-7.0	SSP5-8.5
Research Center for Environmental Changes, Academia Sinica (AS-RCEC)	Tai-ESM1	N/Y	N/N	N/N	Y/Y
Alfred Wegener Institute (AWI)	AWI-CM-1-1-MR	Y/Y	Y/Y	N/N	Y/Y
Beijing Climate Center, China Meteorological Administration (BCC)	BCC-CSM2-MR	Y/Y	Y/Y	Y/Y	Y/Y
Chinese Academy of Meteorological Sciences (CAMS)	CAMS-CSM1-0	Y/Y	Y/Y	Y/Y	Y/Y
LASG, Institute of Atmospheric Physics, Chinese Academy of Sciences (CAS)	FGOALS-f3-L	Y/Y	Y/Y	Y/Y	Y/Y
	FGOALS-g3	Y/Y	Y/Y	Y/Y	Y/Y
Centre for Climate Change Research, Indian Institute of Tropical Meteorology (CCCR-IITM)	IITM-ESM	N/Y	N/N	N/N	Y/Y
Canadian Centre for Climate Modelling and Analysis (CCCma)	CanESM5	Y/Y	Y/Y	Y/Y	Y/Y
	CanESM5-CanOE	Y/Y	Y/Y	N/N	Y/Y
Euro-Mediterranean Centre for Climate Change (CMCC)	CMCC-ESM2	N/Y	N/N	N/Y	Y/Y
	CMCC-CM2-SR5	N/Y	N/N	N/N	Y/Y
Centre National de Recherches Météorologiques/ Centre Européen de Recherche et Formation Avancées en Calcus Scientifique (CNRM-CERFACS)	CNRM-ESM2-1	Y/Y	Y/Y	Y/N	Y/Y
	CNRM-CM6-1	N/N	N/N	N/N	Y/Y
Commonwealth Scientific and Industrial Research Organisation (CSIRO)	ACCESS-ESM1-5	Y/Y	Y/Y	Y/Y	Y/Y
Commonwealth Scientific and Industrial Research Organisation, ARC Centre of Excellence for Climate System Science (CSIRO-ARCCSS)	ACCESS-CM2	Y/Y	Y/Y	Y/Y	Y/Y
EC-Earth-Consortium	EC-Earth3	Y/Y	Y/Y	Y/Y	Y/Y
	EC-Earth3-CC	N/N	N/N	N/N	Y/Y
Energy Exascale Earth System Model Project (E3SM-Project)	E3SM-1-1	N/N	N/N	N/N	Y/Y
First Institution of Oceanography (FIO-QLNM)	FIO-ESM-2-0	Y/Y	Y/Y	N/N	Y/Y
Institute of Numerical Mathematics (INM)	INM-CM4-8	Y/Y	Y/Y	Y/Y	Y/Y
	INM-CM5-0	Y/Y	Y/Y	Y/Y	Y/Y

Earth System
Dynamics
Discussions

Modeling Center (Group)	Model	SSP1-2.6	SSP2-4.5	SSP3-7.0	SSP5-8.5
Institut Pierre Simon Laplace (IPSL)	IPSL-CM6A-LR	Y/Y	Y/Y	Y/Y	Y/Y
Japan Agency for Marine-Earth Science	MIROC6	Y/Y	Y/Y	Y/Y	Y/Y
and Technology/ Atmosphere and Ocean	MIROC-ES2l	Y/Y	Y/Y	Y/Y	Y/Y
Research Institute, University of Tokyo					
(MIROC)					
Met Office Hadley Centre (MOHC)	UKESM1-0-LL	Y/Y	Y/Y	Y/Y	Y/Y
Max Planck Institute for Meteorology	MPI-ESM1-2-LR	Y/Y	Y/Y	Y/Y	Y/Y
(MPI-M)					
Meteorological Research Institute (MRI)	MRI-ESM2-0	Y/Y	Y/Y	Y/Y	Y/Y
National Center for Atmospheric Re-	CESM2	Y/Y	Y/Y	N/N	Y/Y
search (NCAR)	CESM2-WACCM	Y/Y	Y/Y	Y/Y	Y/Y
Norwegian Climate Center (NCC)	NorESM2-MM	Y/Y	Y/Y	Y/Y	Y/Y
National Institute of Meteorological	KACE-1-0-G	Y/Y	Y/Y	N/N	Y/Y
Sciences-Korea Met. Administration					
(NIMS-KMA)					
NOAA Geophysical Fluid Dynamics Lab-	GFDL-CM4	N/N	Y/Y	N/N	Y/Y
oratory (NOAA-GFDL)	GFDL-ESM4	Y/Y	Y/Y	Y/Y	Y/Y
Nanjing University of Information Sci-	NESM3	Y/Y	Y/Y	N/N	Y/Y
ence and Technology (NUIST)					
	Number of models per scenario	26/30	27/27	20/20	34/34

evaluation of the model, we use W5E5 reanalysis data (Lange, 2019) with a native grid of 0.5°longitude x 0.5°latitude grid during the reference period and regrid it to the 1°longitude x 1°latitude grid. This data set is based on the WATCH Forcing Data methodology applied to ERA5 data (WFDE5; Cucchi et al. (2020); Weedon et al. (2011)) and ERA5 reanalysis data (Hersbach et al., 2019, 2020).

3 Results

3.1 Model comparison

To evaluate the models' capacity in capturing the seasonal rainfall of the EASM in the past, we compare the mean seasonal rainfall to W5E5 reanalysis data in the period 1995-2014. The historical rainfall in the reanalysis data is 4.7 ± 0.3 mm/day. While 16 out of 34 models are able to capture the historical mean within plus/minus two standard deviations, 14 models have a

99 tendency to overestimate and 4 models to underestimate the mean (See Fig. 1). The mean of the models range from 3.4 mm/day

100 (CAMS-CSM1-0) to 6.6 mm/day (INM-CM4-8). The models EC-Earth-3 and MPI-ESM1-2-LR capture the mean rainfall best.

101 The standard deviations of the model range from 0.2 mm/day (IITM-ESM) to 0.4 mm/day (INM-CM5-0). In this study, models

102 within two standard deviations are called group A models, the remaining ones group B models. The results in this study are

103 shown for group A models in the Results section, and in the Appendix for group B models.

104 The rainfall during the EAM is strongest along coastal regions, particularly in South and East China, the Korean peninsula,

105 as well as Japan and Taiwan (See Fig. 2). From the 16 group A models, most are able to reproduce major spatial patterns

106 including the rainfall in South China (Fig. 2). Regarding the Korean peninsula and Taiwan, the models have a tendency to

107 underestimate the local rainfall. Japan is captured reasonably well. The results for the individual models are shown in Fig. 3

108 and Fig. A1. Other studies focusing on the model evaluation provide further insides regarding the CMIP6 models' performance

109 for the EASM, e.g. Jiang et al. (2020).

3.2 Seasonal mean rainfall

111 In order to analyse the long-term trend of the EASM under climate change, we provide the time series between 1850-2100 for

112 all models in group A (Fig. 4) under four emission scenarios. Fig. B1 shows the time series averaged over all models including

113 group A and group B. The multi-model mean time series captures the decrease of rainfall in the second half of the 20th century

114 resulting from increasing aerosol pollution. The group A models show a stronger decrease in that time period compared to

115 group B models. This is followed by a rainfall increasing trend in the 21st century in all scenarios. The positive slopes in

116 the scenarios vary, potentially depending on the forcings resulting from the underlying socioeconomic pathway, particularly

117 aerosols and greenhouse gas emissions. High levels of development and the focus on health and environmental concerns in

118 SSP1 and SSP5 result in reduced air pollution emissions in the medium and long term. SSP2 has similar tendencies but

119 slower implementation and SSP3 is characterized by weak aerosol control and slow development of air pollution policies. This

120 explains that rainfall raises slower in SSP3 in the first half of the 21st century compared to other emission scenarios.

121 The time series for individual models under SSP5-8.5 are shown in Fig. 5 for group A and Fig. C1 for group B. Most group

122 A models reproduce the reducing the EASM monsoon rainfall in the second half of the 20th century. In the 21st century, all

123 group A models show a positive rainfall trend. Apart from MIROC-ES2L and CAMS-CSM1-0, also all group B models project

124 increasing rainfall during the 21st century.

125 To analyse the change in rainfall until the end of the 21st century, we calculate the difference in JJA rainfall from 2081-2100

126 compared to the reference period 1995-2014 for the four SSPs. Under SSP5-8.5, SSP3-7.0 and SSP2-4.5 all models project

127 an increase. Under SSP1-2.6, 25 out of 26 models project an increase in EASM rainfall. The increase differs between the

128 underlying emission scenarios: Under SSP5-8.5, the increase is 17.2% for the multi-mean of group A models (12.7% for group

129 B models). The largest increase in group A models is projected by KACE-1-0-G to be 28.7%, the smallest increase is projected

130 by AWI-CM-1-1-MR with 6.% (Fig. 6). Under SSP3-7.0, the group A models project an average increase of 12.7% (8.0% for

131 group B; Fig. 7). Under SSP2-4.5, the increase projected by group A models is 11.9% (8.6% for group B; Fig. 8) and under

132 SSP1-2.6, it is 11.2% (6.6%; Fig. 9). The group A models project stronger increases in the EASM rainfall. Besides, it has to
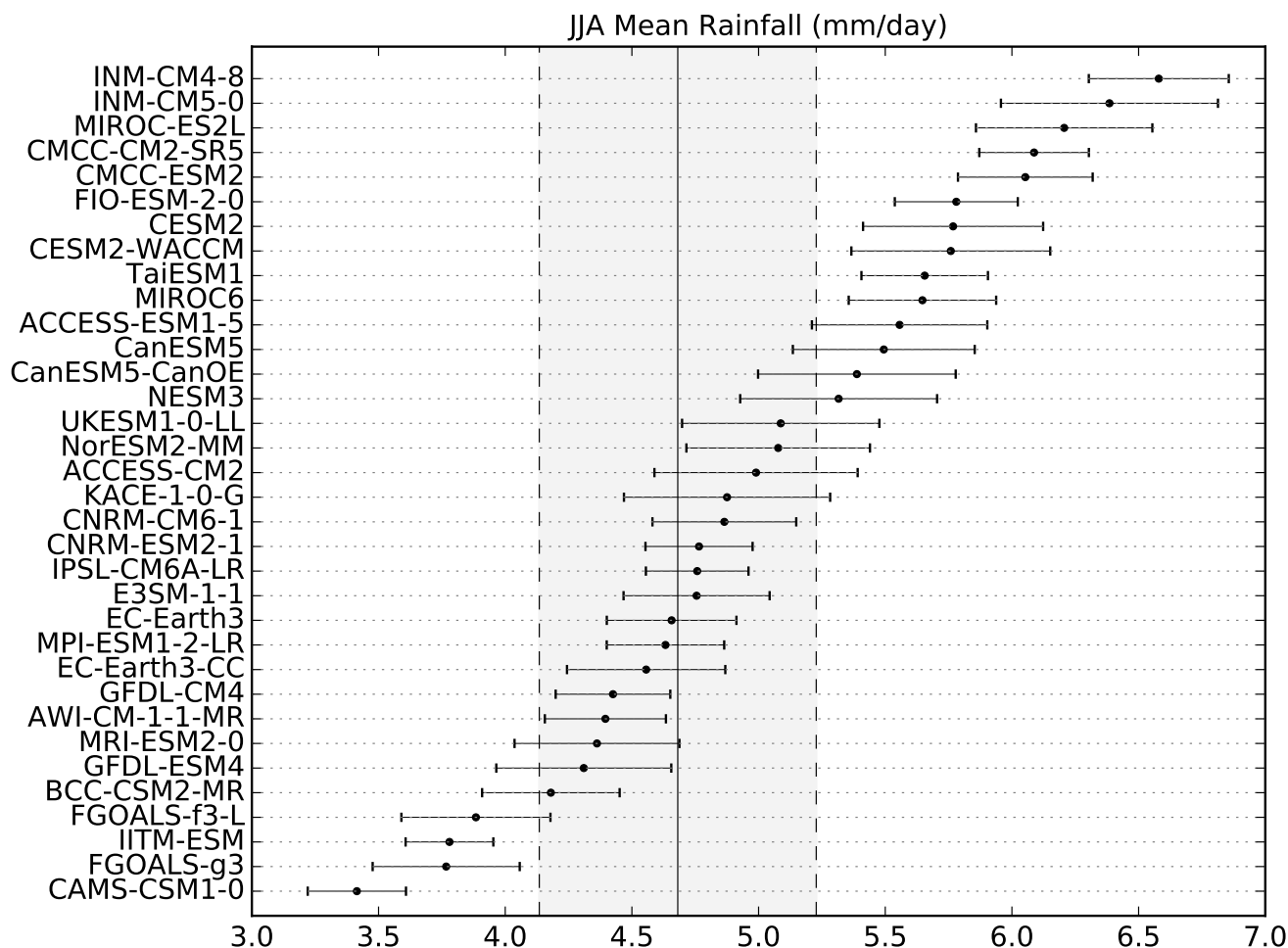
Figure 1. Mean Rainfall of the East Asian Summer Monsoon from June-September (mm day^{-1}) over the region displayed in Fig. A1 from 34 CMIP6 models. The vertical line mark the mean monsoon rainfall from W5E5 renalysis data (continuous line) plus/minus two standard deviations (dashed line). Circles with error bars represent mean plus/minus one standard deviation for each individual climate model during the same period.
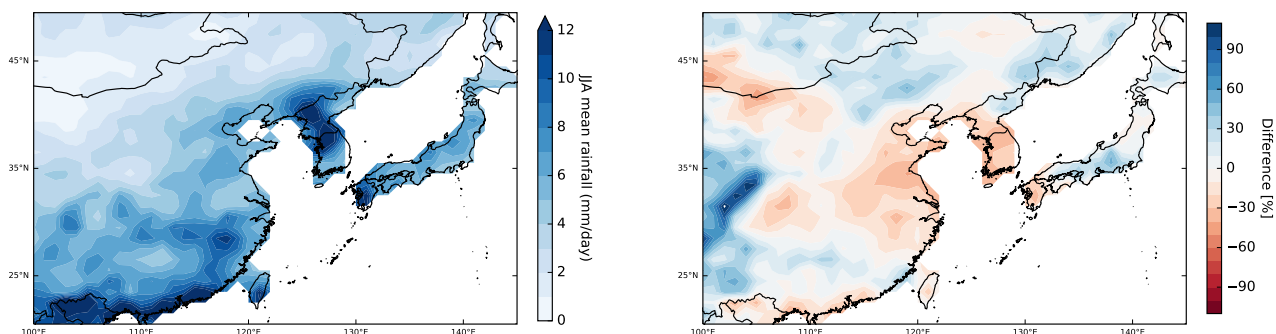
Figure 2. Left: Spatial distribution of EAM averaged over the period 1995-2014 from W5E5 reanalysis data. Right: Difference [%] between reanalysis data and multi-model-mean of the 16 group A models for the same time period.
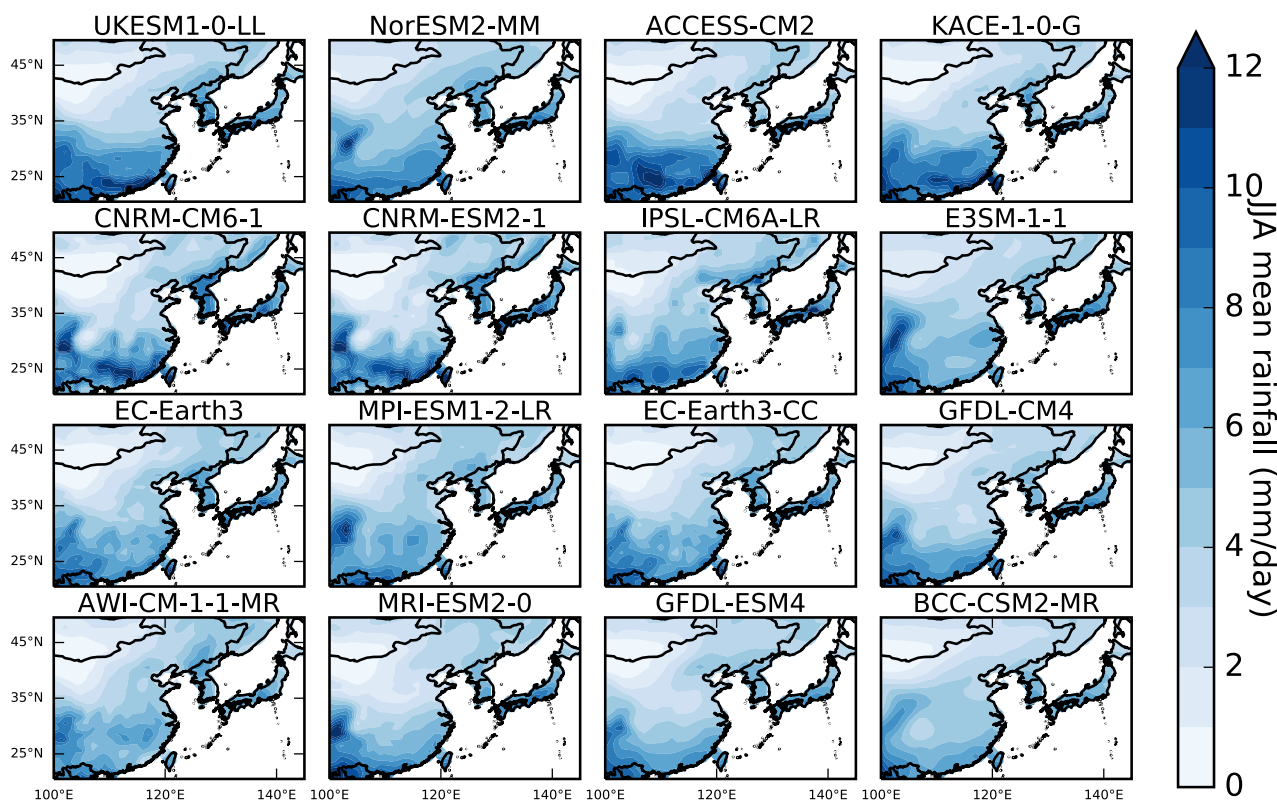
Figure 3. Spatial distribution of EASM averaged over the period 1995-2014 from the 16 models in group A.

Earth System
Dynamics
Discussions

Open Access

133 be noted that the projections of all scenarios lie within the uncertainty ranges of the other scenarios. Further details regarding

134 other periods (2021-2040, 2041-2060, 2061-2080) can be found in Table 2. Regarding the monsoon change only over China,

135 the increase projected by group A models is even stronger: Under SSP1-2.6 the monsoon rainfall intensifies by 12.1%, under

136 SSP2-4.5 by 12.7%, under SSP3-7.0 by 14.1% and under SSP5-8.5 by 19.1% in multi-model average.

137 The spatial change in EASM rainfall between 2081-2100 and 1995-2014 based on the group A multi-model mean is shown

138 in Fig. 10 for SSP5-8.5. The rainfall in the entire EASM region is projected to increase in multi-model mean, particularly in

139 Taiwan, South-East China as well as North Korea and adjacent regions. The majority of group A models coincide in the larger

140 scale rainfall change pattern. Though, some models project regional decrease of rainfall in different areas (Fig. D1). The results

141 for group B models are shown in Fig. E1. Fig. F1 shows the multi-model mean of spatial changes for the EASM under the four

142 different scenarios only for the models that are available for all four scenarios. The regions with intensifying rainfall coincide

143 with the areas under SSP5-8.5, though the intensity varies according to the underlying forcing.

144 Besides, we analyse the dependence of EASM rainfall on global mean temperature (GMT). The multi-model mean indicates

145 a linear relationship relatively independent of the underlying emission scenario (Fig. 11). The projected average increase

146 in daily rainfall during the monsoon season is 0.14mm per degree of global warming. This refers to an increase in EASM

147 rainfall of 3.0% (1.4-4.6%) per degree GMT increase. The increase ranges from 0.06mm/day to 0.22mm/day depending on the

148 providing model.

Table 2. Multi-model mean changes [%] in JJA rainfall from different future periods compared to reference period 1995-2014 (group A/ group B/ all).

Scenario	2021-2040	2041-2060	2061-2080	2081-2100
SSP1-2.6	4.7/2.9/3.7	8.3/5.5/6.8	10.2/6.0/7.9	11.2/6.6/8.8
SSP2-4.5	4.9/2.0/3.4	7.8/4.7/6.2	9.1/6.2/7.6	11.9/8.6/10.2
SSP3-7.0	3.4/0.3/1.9	5.4/2.4/3.9	9.4/4.0/6.7	12.7/8.0/10.4
SSP5-8.5	5.9/2.6/4.2	9.2/5.3/7.1	13.0/8.6/10.7	17.2/12.7/14.8

149 ### 3.3 Interannual variability

150 Furthermore, we analyse the interannual variability of the EASM rainfall. For this purpose, we remove the nonlinear trend

151 obtained by the singular spectrum analysis (see Fig. 5 and C1). We use the percentage changes in standard deviation between

152 2050-2100 and 1965-2015. Under SSP5-8.5, 15 of the 16 group A models project an increase of interannual variability with a

153 multi-mean of 31.4% ranging from -1.5% to 31.4% (Fig. 12). Under SSP3-7.0, 7/10 group A models project an increase with

154 an average of 10.6% (-20.0% to 34.3%; Fig. G1). Under SSP2-4.5, 10/13 project increasing variability of 10.4% (-14.0% to

155 30.8%;Fig. H1) and under SSP1-2.6, an increase is projected by 7/12 group A models with a multi-model average of 7.0%

156 (-24.8% to 27.5%; Fig. I1). With stronger emission scenarios, the increase of interannual variability is stronger with more

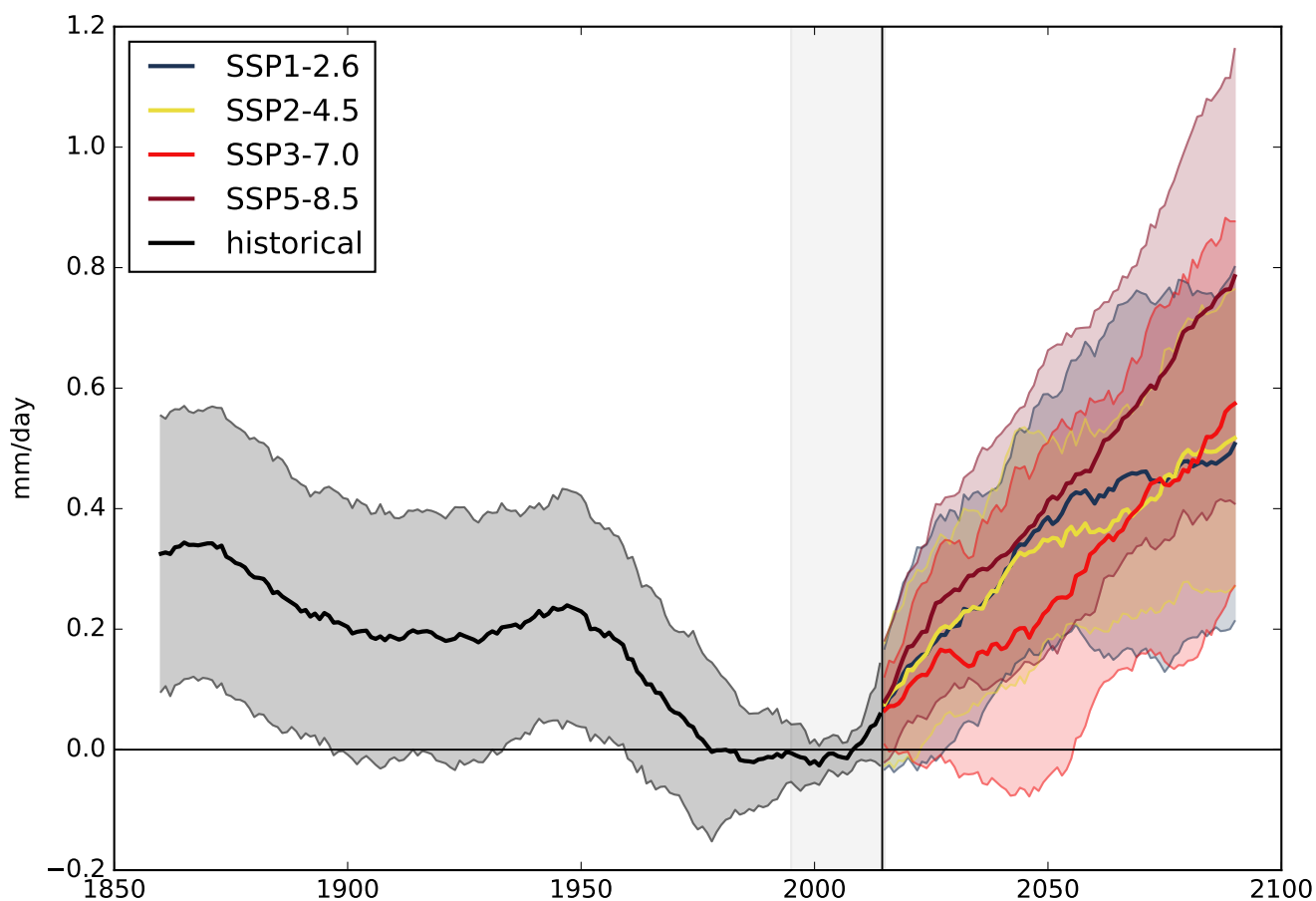157 models coinciding in the sign of the change.

Figure 4. Time series of EASM (mm d^{-1}) for the period 1850-2100 based on the multi-model mean of the 16 models in group A relative to the period 1995-2014. The time series is based on the 20-years-running-mean of the individual models. The shading marks the range of plus/minus one standard deviation. Availability of the models in accordance with Table 1.

3.4 Extremely wet seasons

We use the 90th percentile for the period 1965-2015 in order to define extremely wet monsoon seasons. Thus, per definition 5 out of 50 years were extremely wet during the 50-years period from 1965-2015. Under SSP5-8.5, the number of extremely wet monsoon seasons will increase by a factor of 6.5 until 2050-2100. Respectively, 32.4 years are expected to be extremely wet in 2050-2100 with individual group A model projections ranging from 14 to 46 out of 50 seasons. Under SSP3-7.0, the multi-model mean projection is 26.1 ranging from 7 to 41 extremely wet seasons. Under SSP2-4.5, 25.5 seasons in the future period are projected to be extremely wet ranging from 7 to 36 and under SSP1-2.6 the multi-model mean projection is 25.6 ranging from 8 to 37 seasons. The increase over time is shown in Fig. 13.
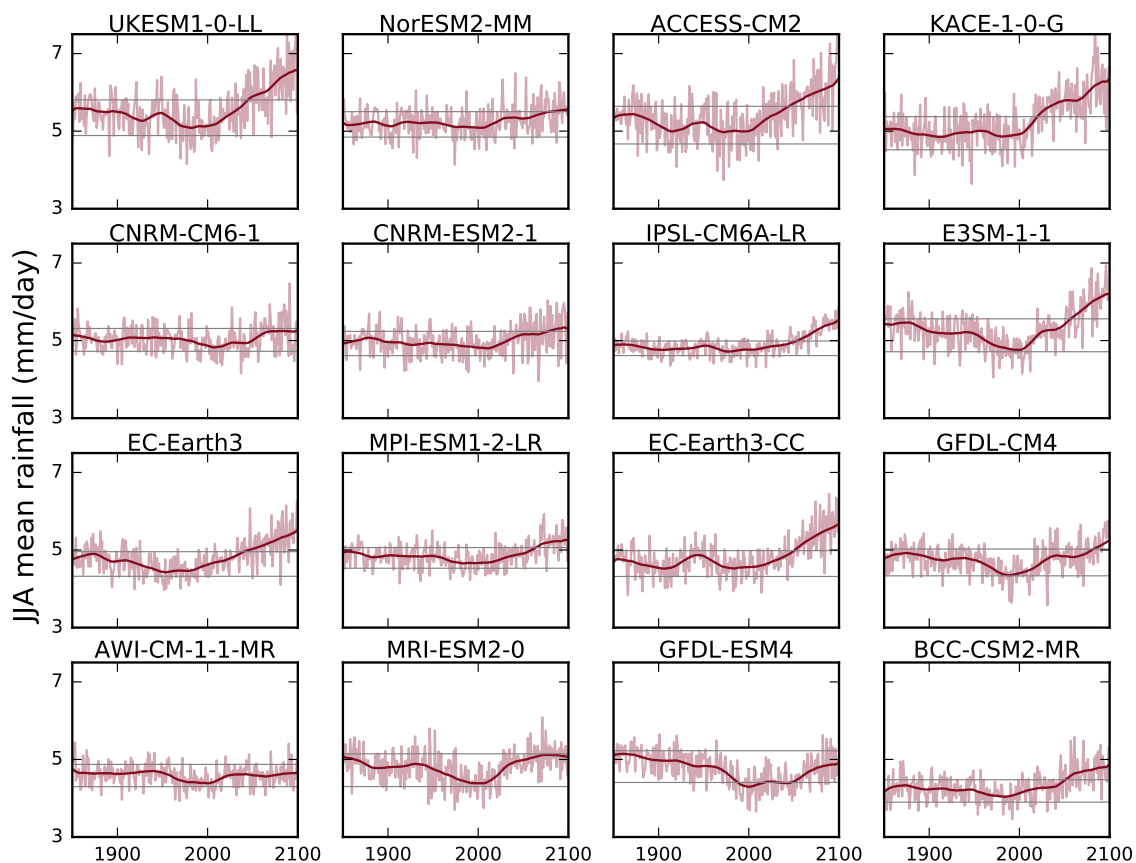
Figure 5. Time series of EASM (mm/day) for the period 1850-2100 from the 16 models in group A. Light red lines represent the annual values; red lines mark the trend obtained from a singular spectrum analysis with a window size of 20 years. For the method, see Golyandina and Zhigljavsky (2013). The horizontal grey lines represent mean $\pm$ standard deviation for each model for the period 1850-2015.
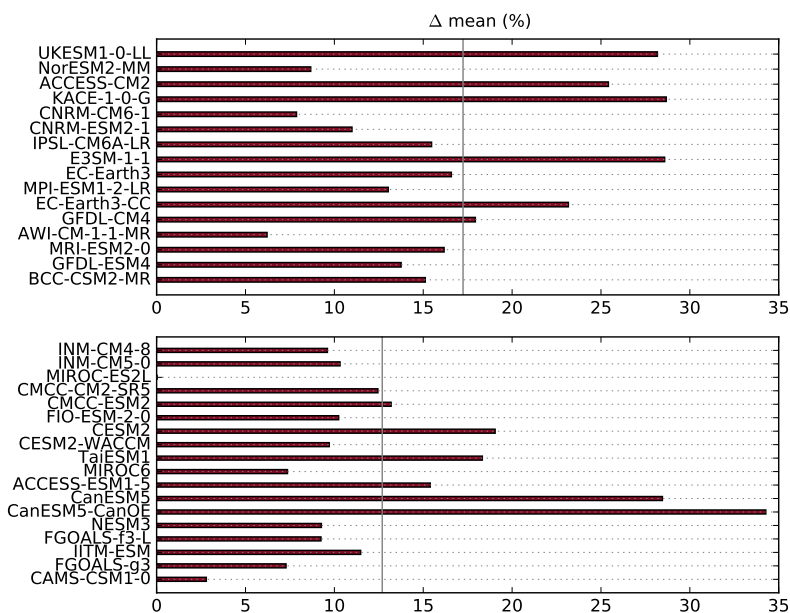
Figure 6. Changes [%] in JJA rainfall between 2081-2100 and 1995-2014 under SSP5-8.5. Upper panel shows group A models, the lower panel group B models. The vertical line marks the multi-model-mean for both groups.
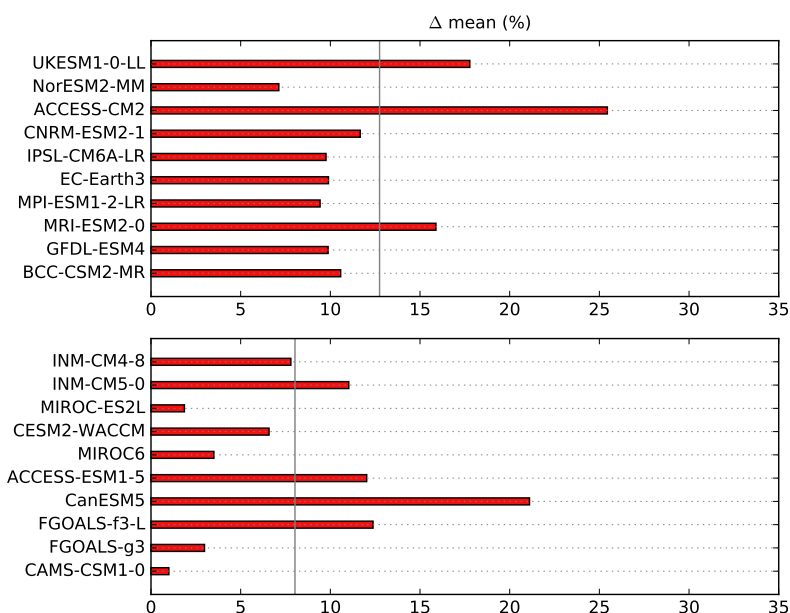
Figure 7. Changes [%] in JJA rainfall between 2081-2100 and 1995-2014 under SSP3-7.0. Upper panel shows group A models, the lower panel group B models. The vertical line marks the multi-model-mean for both groups.
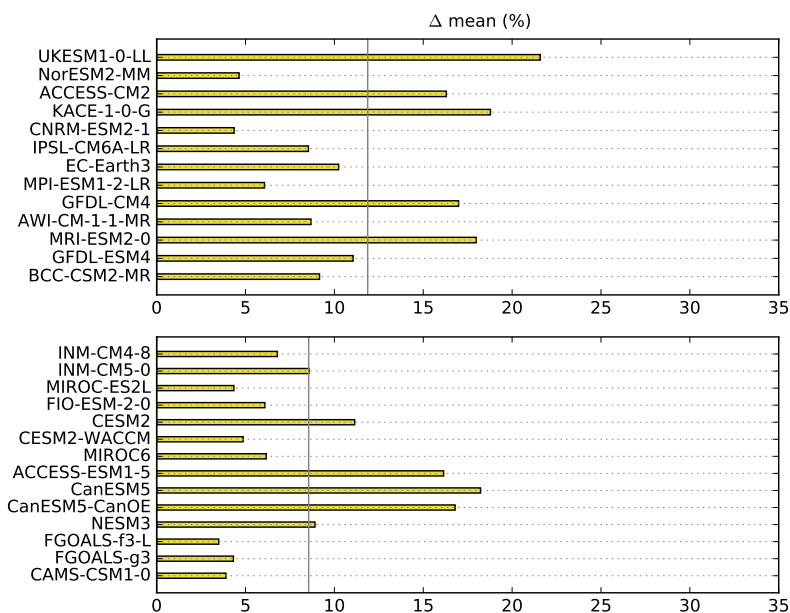
Figure 8. Changes [%] in JJA rainfall between 2081-2100 and 1995-2014 under SSP2-4.5. Upper panel shows group A models, the lower panel group B models. The vertical line marks the multi-model-mean for both groups.
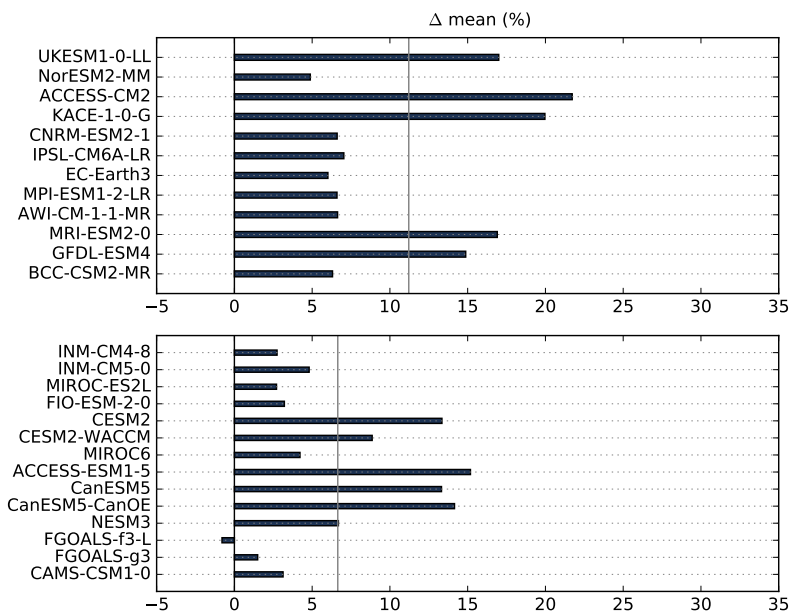
Figure 9. Changes [%] in JJA rainfall between 2081-2100 and 1995-2014 under SSP1-2.6. Upper panel shows group A models, the lower panel group B models. The vertical line marks the multi-model-mean for both groups.
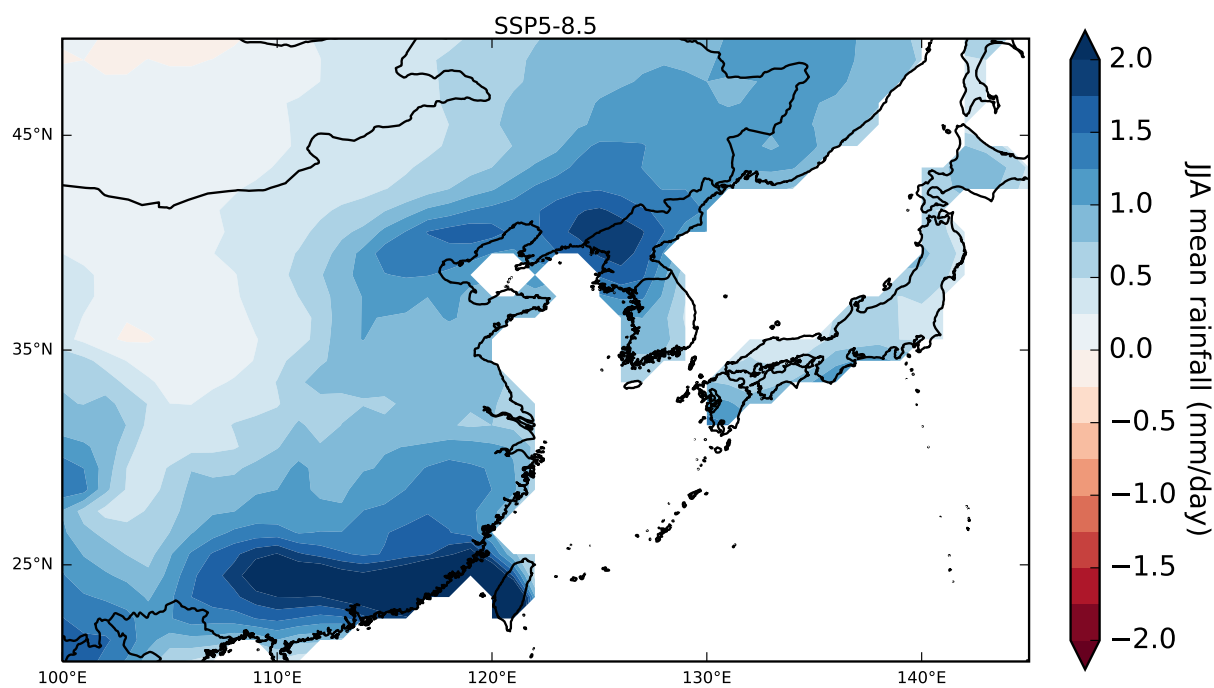
Figure 10. Spatial changes in JJA rainfall between 2081-2100 and 1995-2014 under SSP5-8.5 for multi-modeal mean of group A models. The individual model results are shown in Fig. D1 and Fig. E1.
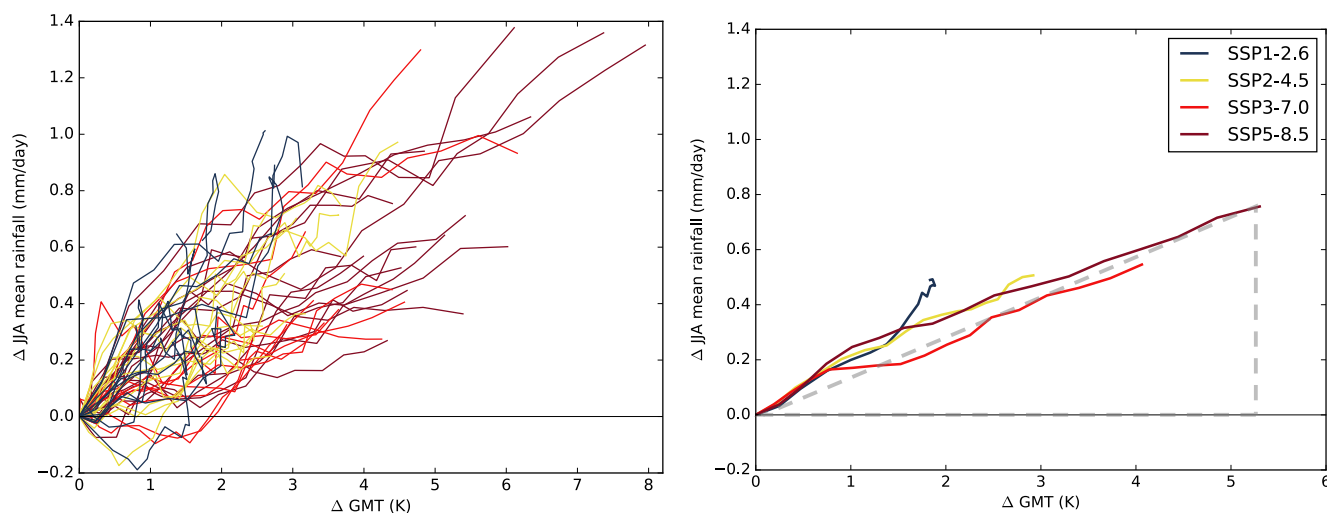
Figure 11. Change of EASM rainfall (mm/day) depending on change in global mean temperature (K) during the 21st century for all group A models (left) and their multi-model average (right). The change is shown based on 20-year periods (1995-2015, 2000-2020, 2005-2025,...). Dashed gray lines indicate the slope. The reference period is 1995-2014.
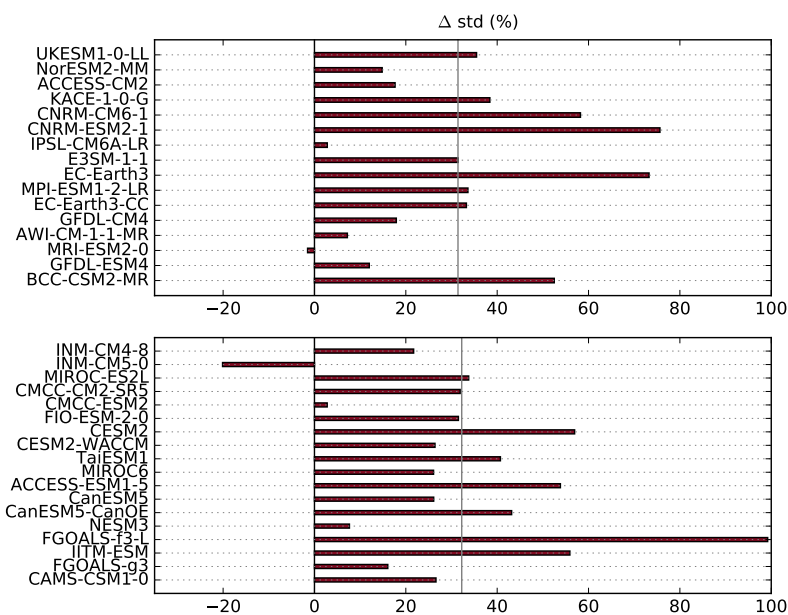
Figure 12. Change [%] of interannual variability between 2050-2100 and 1965-2015 for the EASM seasonal rainfall under SSP5-8.5. The upper panels show the group A models, the lower panels the group B models. The vertical line indicates the multi-model mean of the respective group.
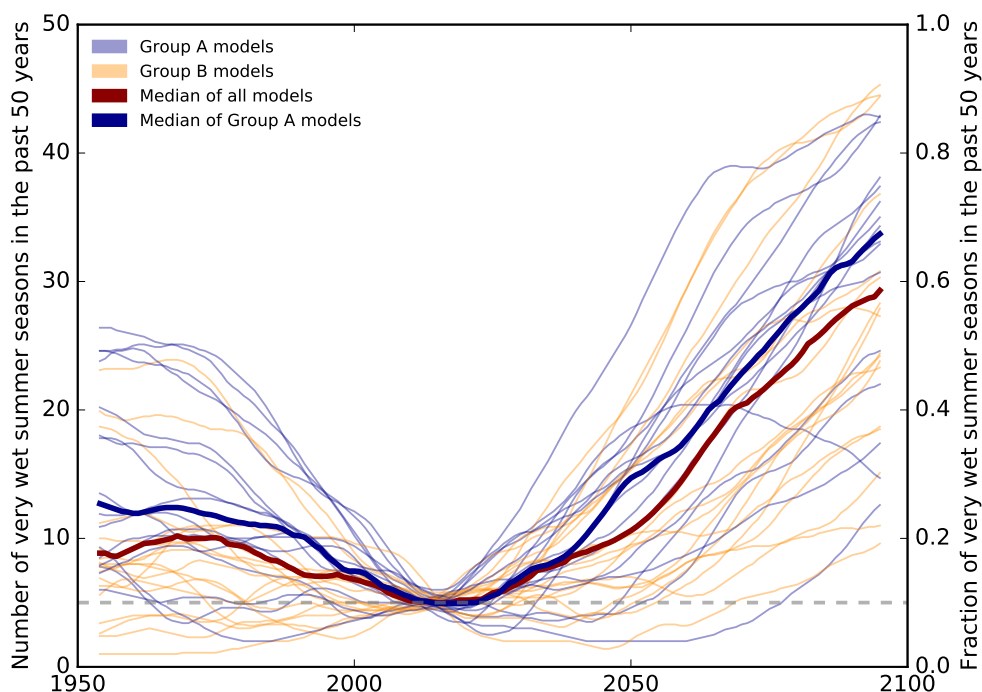
Figure 13. Increase of extremely wet monsoon seasons under unabated climate change (SSP5-8.5). Group A models are shown in blue, group B models in orange. The reference period is 1965-2015 where per definition 5 out of 50 years were extremely wet.

4   Discussion and Conclusion

In this study, we use 34 CMIP6 models in order to analyse their future projections under climate change regarding the East Asian Summer Monsoon. We identify models that capture the rainfall in 1995-2014 within two standard deviations as group A models and use them for our main analysis. The CMIP6 models have a tendency to overestimate the EASM rainfall which is in line with previous studies (Jiang et al., 2020). This is different from other Asian monsoon regions, e.g. in the Indian monsoon region models tend to underestimate the seasonal rainfall (Katzenberger et al., 2021, 2022). All group A models robustly project an increase of rainfall under all four emission scenarios. The projected multi-model mean increase until 2081-2100 is 17.2% under SSP5-8.5, 12.7% under SSP3-7.0, 11.9% under SSP2-4.5 and 11.2% under SSP1-2.6. The rainfall-intensifying tendency is also confirmed by the IPCC, AR6 classifying the increasing trend as 'highly certain' (Masson-Delmotte et al., 2021). The projected increase is also in line with CMIP5 projections, though even stronger increases are projected in CMIP6 (Qu et al., 2014; Chen and Sun, 2013; Kitoh et al., 2013). But it has to be noted, that there are differences in the methods between the studies, preventing direct comparison of the results. The projections for the near-term depend on the implementation and

178 efficiency of future air pollution control that is difficult to predict (Wilcox et al., 2020) adding uncertainty mainly for the period

179 2021-2040. The increase in rainfall will particularly contribute to rainfall in South East China, Taiwan as well as North Korea -

180 regions that are already experiencing a relatively strong monsoon. Thus the wet-regions-get-wetter dynamics is predominantly

181 confirmed for the EASM in line with CMIP5 results (Seo et al., 2013). Over China, the monsoon is projected to increase

182 by 12.1% under SSP1-2.6, under SSP2-4.5 by 12.7%, under SSP3-7.0 by 14.1% and under SSP5-8.5 by 19.1%. Per degree

183 of global warming, the monsoon is projected to increase by 0.14mm/day which refers to 3% of the rainfall in the reference

184 period. The intensification of the EASM is resulting from the combined effects of an enhanced evaporation due to increased

185 sea surface temperatures, increased water vapour as well as moist flux convergence induced by the (north) westward shift of

186 the North Pacific subtropical high (Seo et al., 2013; Qu et al., 2014). Additionally, the strengthening of the land-sea thermal

187 contrast under global warming contributes to the rainfall increase of Asian monsoon systems (Endo et al., 2018).

188 Besides, we analysed the interannual variability that is particularly important for societal and economic adaptation strategies,

189 defining the necessary interannual flexibility for agricultural irrigation, flooding management, etc. The interannual variability

190 is projected to increase by 7.0% under SSP1-2.6, 10.4% under SSP2-4.5, 10.5% under SSP3-7.0 and 31.4% under SSP5-8.5

191 from 1965-2015 to 2050-2100. Comparing the CMIP6 multi-mean results under SSP5-8.5 of 31.4% to CMIP3 results under

192 the respective A2 scenario, the projected increase in CMIP3 of 19% is considerably weaker (Lu and Fu, 2010). Additionally,

193 extremely wet monsoon seasons are projected to occur 6.5 times more often under SSP5-8.5 compared to the reference period.

194 The increase of interannual variability of the seasonal rainfall is accompanied by increasing interannual variability of the

195 western North Pacific subtropical high and East Asian upper-tropospheric jet (Lu and Fu, 2010). The projected changes in

196 the characteristics of the EASM are of high socioeconomic relevance and should be taken into account in the management
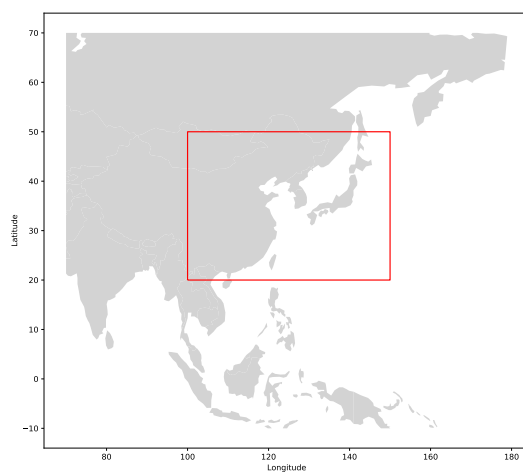
197 decisions for the 21st century.

Figure A1. Area of the East Asian summer monsoon from 20-50°N and 100-150°E as covered in this study.

Earth System
Dynamics
Discussions

Table A1. Overview of the model resolutions of the native model grids in which the 34 CMIP models were run. For the analysis in this study, the models have been remapped to a 1°horizontal grid.

Model	Atmosphere [km]	Land [km]	Ocean [km]
Tai-ESM1	100	100	100
AWI-CM-1-1-MR	100	100	25
BCC-CSM2-MR	100	100	50
CAMS-CSM1-0	100	100	100
FGOALS-f3-L	100	100	100
FGOALS-g3	250	250	100
IITM-ESM	250	250	100
CanESM5	500	500	100
CanESM5-CanOE	500	500	100
CMCC-ESM2	100	100	100
CMCC-CM2-SR5	100	100	100
CNRM-ESM2-1	250	250	100
CNRM-CM6-1	250	250	100
ACCESS-ESM1-5	250	250	100
ACCESS-CM2	250	250	100
EC-Earth3	100	100	100
EC-Earth3-CC	100	100	100
E3SM-1-1	100	100	50
FIO-ESM-2-0	100	100	100
INM-CM4-8	100	100	100
INM-CM5-0	100	100	50
IPSL-CM6A-LR	250	250	100
MIROC6	250	250	100
MIROC-ES2l	500	500	100
UKESM1-0-LL	250	250	100
MPI-ESM1-2-LR	250	250	250
MRI-ESM2-0	100	100	100
GISS-E2-1-G	250	250	100
CESM2	100	100	100
CESM2-WACCM	100	100	100

Earth System
Dynamics

Discussions

Table A1. Continued.

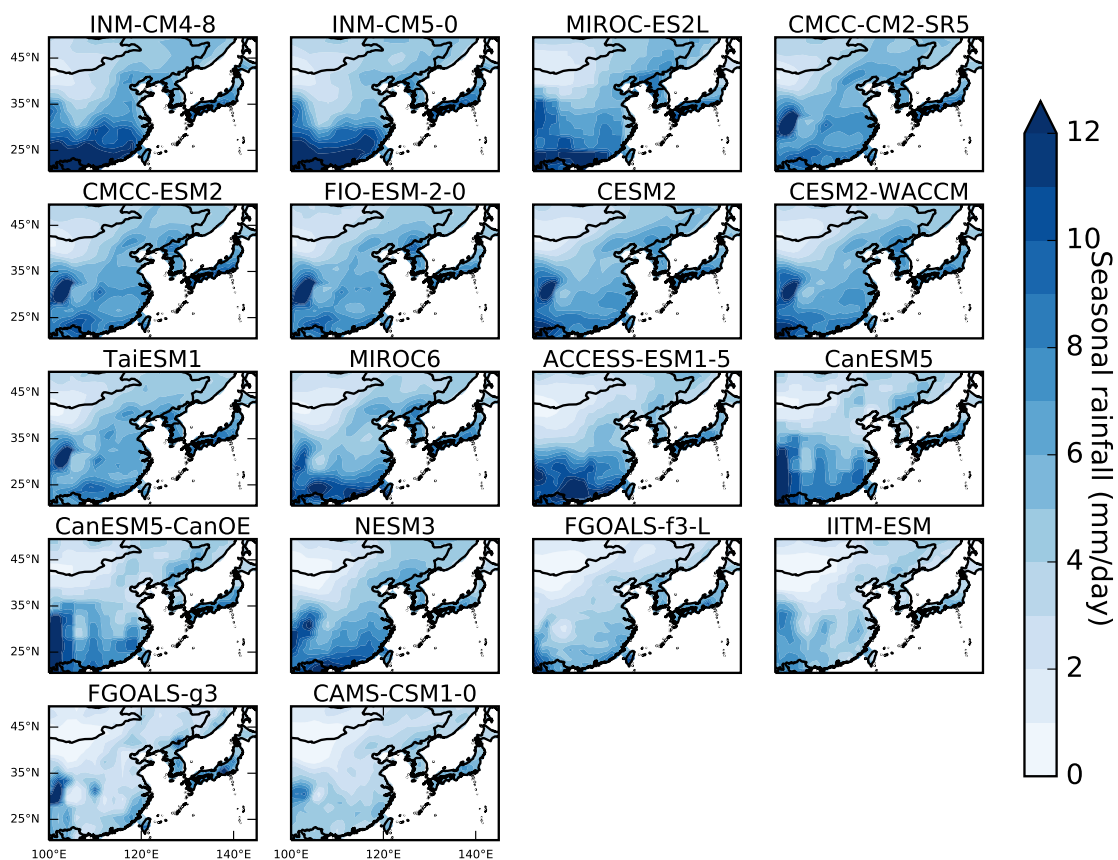| Model	Atmosphere [km]	Land [km]	Ocean [km]
NorESM2-MM	100	100	100
KACE-1-0-G	250	250	100
GFDL-CM4	100	100	25
GFDL-ESM4	100	100	50
NESM3	250	2.5	100

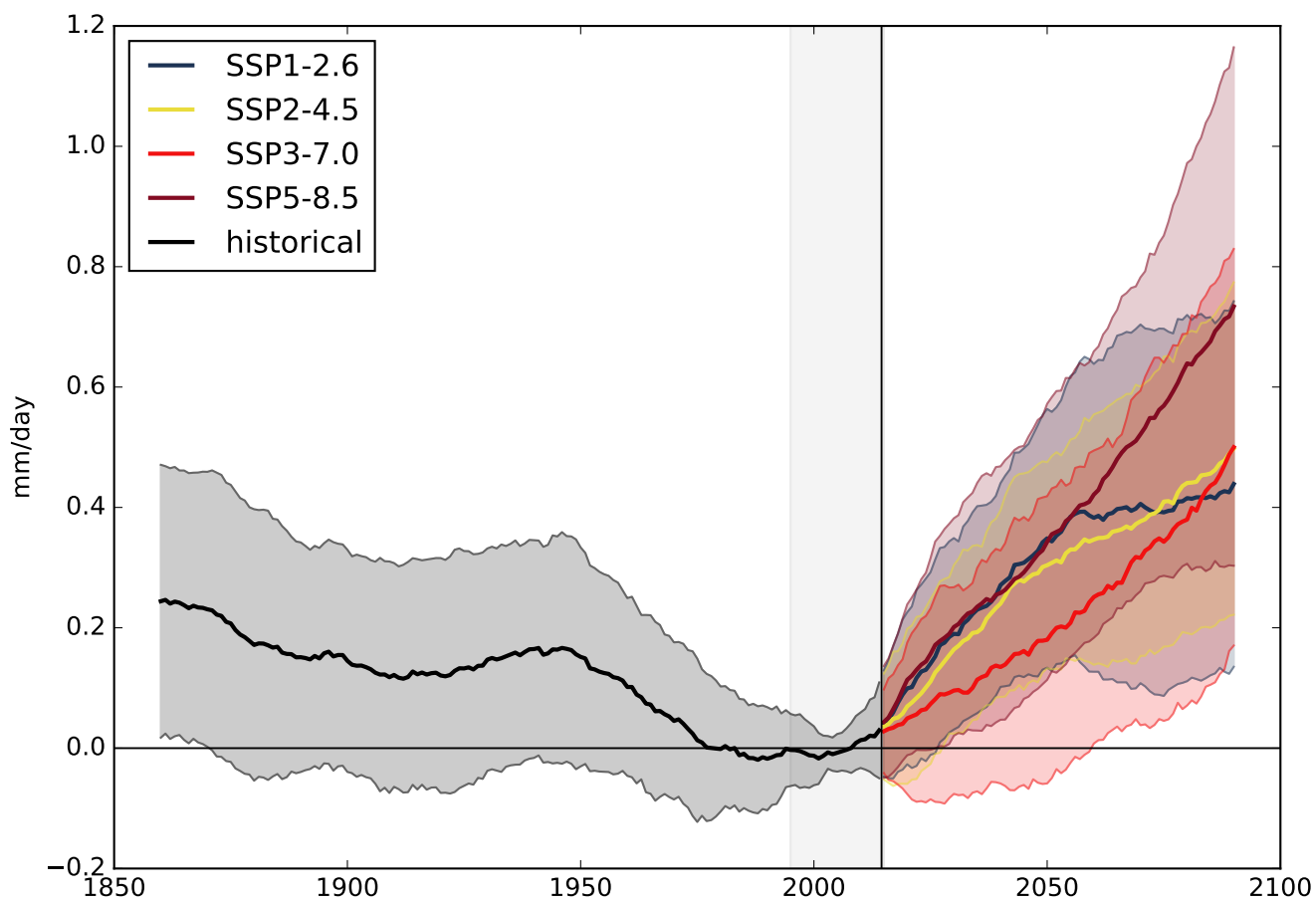**Figure A1.** Spatial distribution of EAM averaged over the period 1995-2014 from the 18 models in group B.

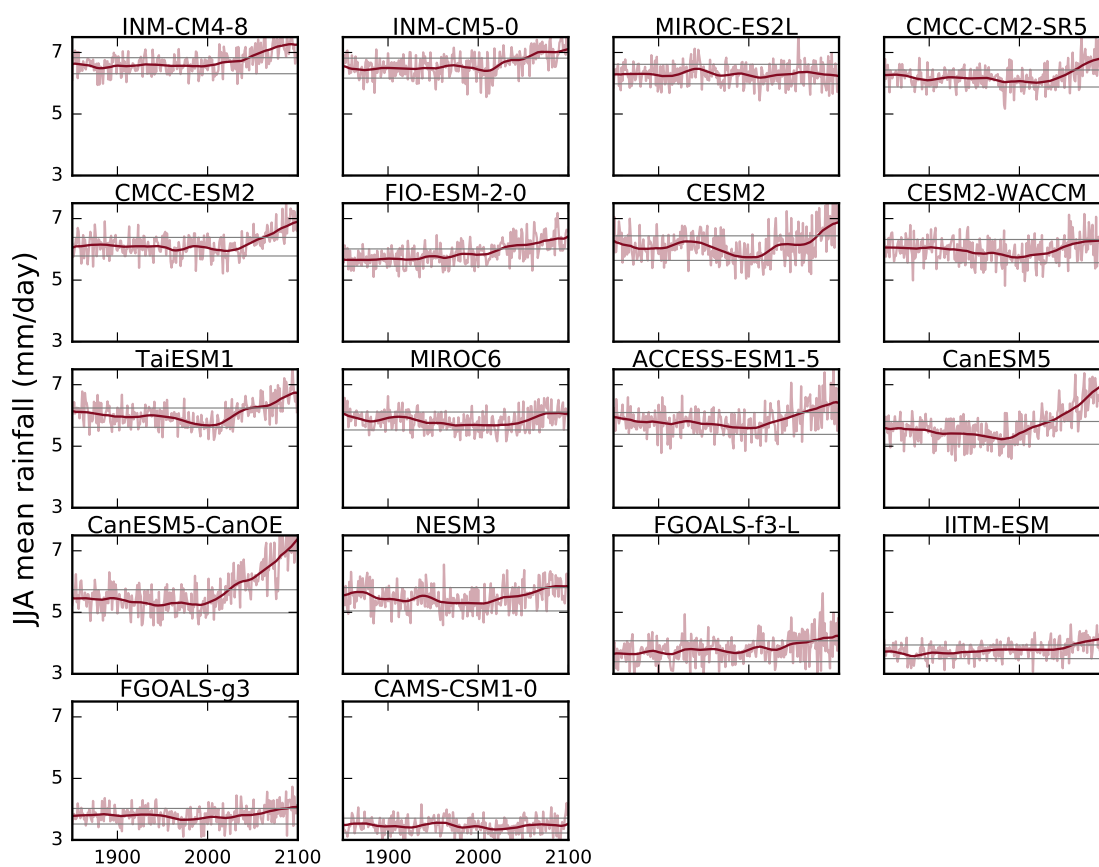**Figure B1.** As in Fig. 4 but including all 34 models from group A and B.

Figure C1. As in Fig. 5 but for the models in Group B.
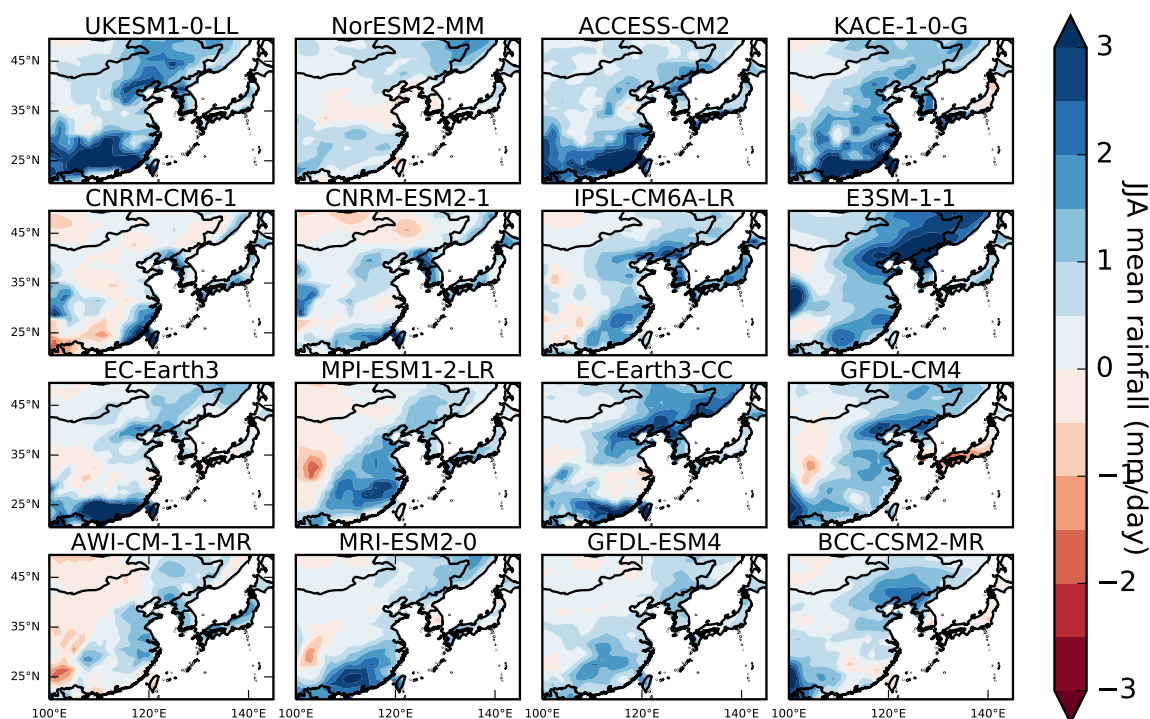
Figure D1. Spatial changes in JJA rainfall between 2081-2100 and 1995-2014 under SSP5-8.5 for group A models. The multi-model mean is shown in Fig. 10.
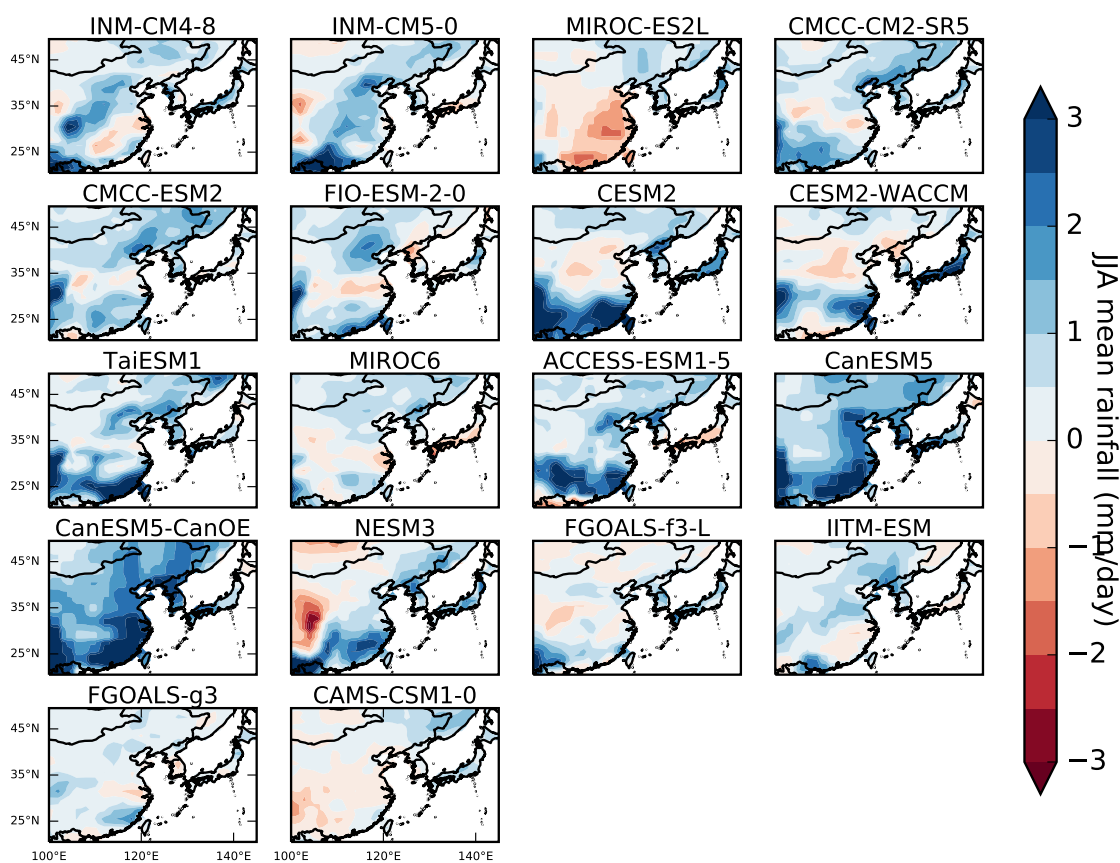
Figure E1. Spatial changes in JJA rainfall between 2081-2100 and 1995-2014 under SSP5-8.5 for group B models.
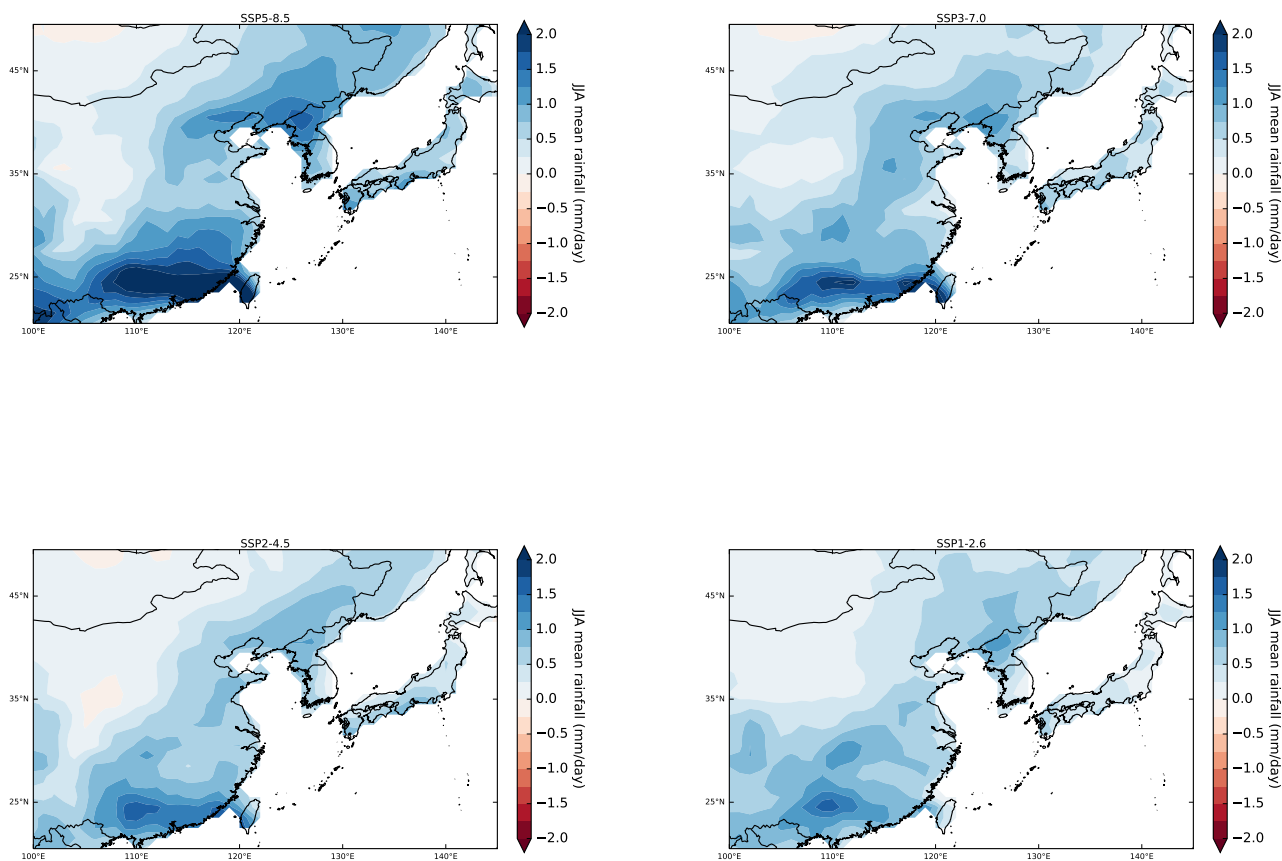
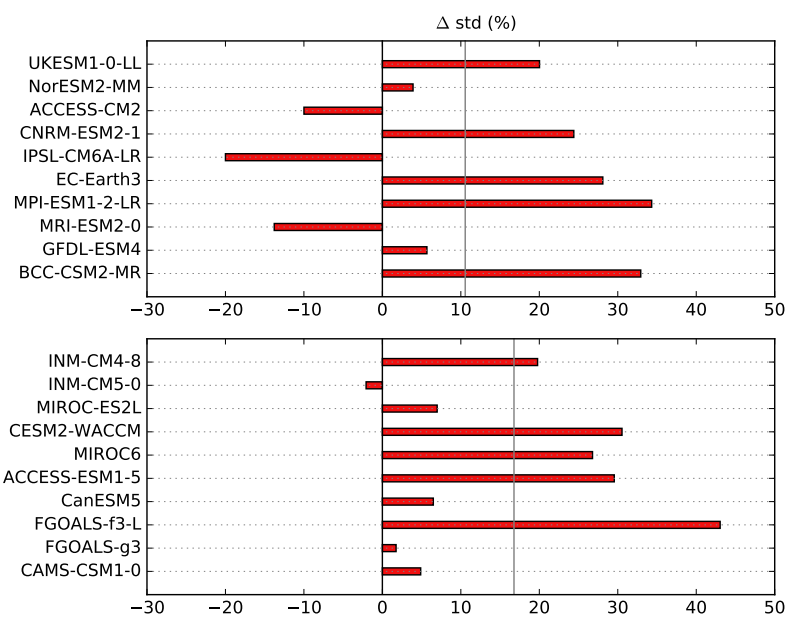**Figure F1.** As in Fig. 10, but using only the group A models that are available for all four scenarios.

Figure G1. Change [%] of interannual variability between 2050-2100 and 1900-1950 for the EASM seasonal rainfall under SSP3-7.0. The upper panels show the group A models, the lower panels the group B models. The vertical line indicates the multi-model mean of the respective group.
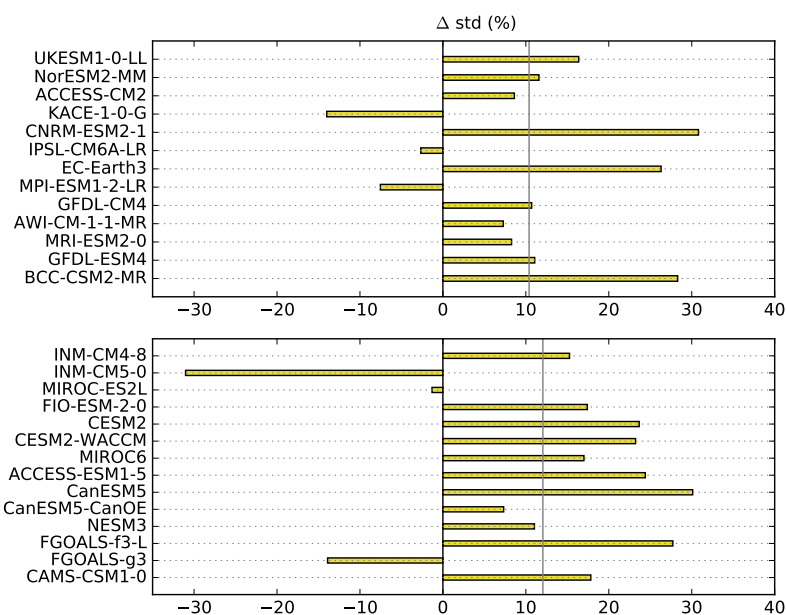
Figure H1. Change [%] of interannual variability between 2050-2100 and 1900-1950 for the EASM seasonal rainfall under SSP2-4.5. The upper panels show the group A models, the lower panels the group B models. The vertical line indicates the multi-model mean of the respective group.
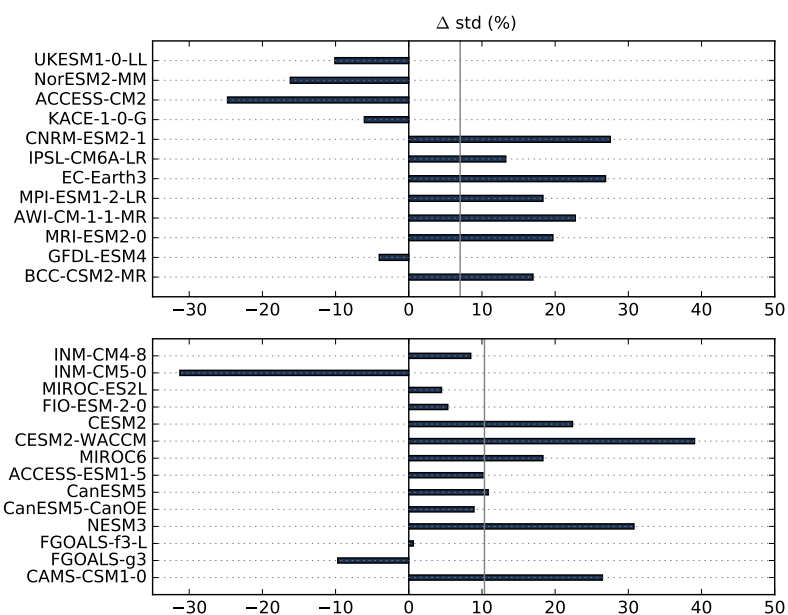
Figure I1. Change [%] of interannual variability between 2050-2100 and 1900-1950 for the EASM seasonal rainfall under SSP1-2.6. The upper panels show the group A models, the lower panels the group B models. The vertical line indicates the multi-model mean of the respective group.

Earth System
Dynamics
Discussions

Open Access

EGU

Statements and Declarations

Author contributions. AL proposed the idea of this study. AK performed the analysis and wrote the paper. AK and AL discussed the results and approved the final version.

Competing interests. At least one of the (co-)authors is a member of the editorial board of Earth System Dynamics. The peer-review process was guided by an independent editor, and the authors have also no other competing interests to declare.

Earth System
Dynamics
Discussions

References

Chen, H. and Sun, J.: Projected change in East Asian summer monsoon precipitation under RCP scenario, Meteorology and Atmospheric Physics, 121, 55–77, 2013.

Chen, Z., Zhou, T., Zhang, L., Chen, X., Zhang, W., and Jiang, J.: Global land monsoon precipitation changes in CMIP6 projections, Geophysical Research Letters, 47, e2019GL086 902, 2020.

Cucchi, M., Weedon, G. P., Amici, A., Bellouin, N., Lange, S., Müller Schmied, H., Hersbach, H., and Buontempo, C.: WFDE5: bias-adjusted ERA5 reanalysis data for impact studies, Earth System Science Data, 12, 2097–2120, https://doi.org/10.5194/essd-12-2097-2020, 2020.

Endo, H., Kitoh, A., and Ueda, H.: A unique feature of the Asian summer monsoon response to global warming: The role of different land–sea thermal contrast change between the lower and upper troposphere, Sola, 14, 57–63, 2018.

Golyandina, N. and Zhigljavsky, A.: Singular Spectrum Analysis for time series, Springer Science & Business Media, 2013.

Ha, K.-J., Heo, K.-Y., Lee, S.-S., Yun, K.-S., and Jhun, J.-G.: Variability in the East Asian monsoon: A review, Meteorological Applications, 19, 200–215, 2012.

Ha, K.-J., Moon, S., Timmermann, A., and Kim, D.: Future changes of summer monsoon characteristics and evaporative demand over Asia in CMIP6 simulations, Geophysical Research Letters, 47, e2020GL087 492, 2020.

Hersbach, H., Bell, B., Berrisford, P., Horányi, A., Sabater, J. M., Nicolas, J., Radu, R., Schepers, D., Simmons, A., Soci, C., et al.: Global reanalysis: goodbye ERA-Interim, hello ERA5, ECMWF newsletter, 159, 17–24, 2019.

Hersbach, H., Bell, B., Berrisford, P., Hirahara, S., Horányi, A., Muñoz-Sabater, J., Nicolas, J., Peubey, C., Radu, R., Schepers, D., Simmons, A., Soci, C., Abdalla, S., Abellan, X., Balsamo, G., Bechtold, P., Biavati, G., Bidlot, J., Bonavita, M., De Chiara, G., Dahlgren, P., Dee, D., Diamantakis, M., Dragani, R., Flemming, J., Forbes, R., Fuentes, M., Geer, A., Haimberger, L., Healy, S., Hogan, R. J., Hólm, E., Janisková, M., Keeley, S., Laloyaux, P., Lopez, P., Lupu, C., Radnoti, G., De Rosnay, P., Rozum, I., Vamborg, F., Villaume, S., and Thépaut, J.-N.: The ERA5 global reanalysis, Quarterly Journal of the Royal Meteorological Society, 146, 1999–2049, https://doi.org/10.1002/qj.3803, 2020.

Huang, D., Liu, A., Zheng, Y., and Zhu, J.: Inter-Model Spread of the Simulated East Asian Summer Monsoon Rainfall and the Associated Atmospheric Circulations From the CMIP6 Models, Journal of Geophysical Research: Atmospheres, 127, e2022JD037 371, 2022.

Huang, D.-Q., Zhu, J., Zhang, Y.-C., and Huang, A.-N.: Uncertainties on the simulated summer precipitation over Eastern China from the CMIP5 models, Journal of Geophysical Research: Atmospheres, 118, 9035–9047, 2013.

Jiang, D., Hu, D., Tian, Z., and Lang, X.: Differences between CMIP6 and CMIP5 models in simulating climate over China and the East Asian monsoon, Advances in Atmospheric Sciences, 37, 1102–1118, 2020.

Kai, T., Zhong-Wei, Y., Xue-Bin, Z., and Wen-Jie, D.: Simulation of precipitation in monsoon regions of China by CMIP3 models, Atmospheric and Oceanic Science Letters, 2, 194–200, 2009.

Katzenberger, A., Schewe, J., Pongratz, J., and Levermann, A.: Robust increase of Indian monsoon rainfall and its variability under future warming in CMIP6 models, Earth System Dynamics, 12, 367–386, 2021.

Katzenberger, A., Levermann, A., Schewe, J., and Pongratz, J.: Intensification of very wet monsoon seasons in India under global warming, Geophysical Research Letters, p. e2022GL098856, 2022.

Kitoh, A., Endo, H., Krishna Kumar, K., Cavalcanti, I. F., Goswami, P., and Zhou, T.: Monsoons in a changing world: A regional perspective in a global context, Journal of Geophysical Research: Atmospheres, 118, 3053–3065, 2013.

Lange, S.: WFDE5 over land merged with ERA5 over the ocean (W5E5). V. 1.0. GFZ Data Services., 2019.

Earth System
Dynamics
Discussions

EGU

Open Access

248 Lee, J.-Y. and Wang, B.: Future change of global monsoon in the CMIP5, Climate Dynamics, 42, 101–119, https://doi.org/10.1007/s00382-
249   012-1564-0, 2014.

250 Lei, Y., Hoskins, B., and Slingo, J.: Exploring the interplay between natural decadal variability and anthropogenic climate change in summer
251   rainfall over China. Part I: Observational evidence, Journal of Climate, 24, 4584–4599, 2011.

252 Lu, R. and Fu, Y.: Intensification of East Asian summer rainfall interannual variability in the twenty-first century simulated by 12 CMIP3
253   coupled models, Journal of Climate, 23, 3316–3331, 2010.

254 Masson-Delmotte, V., P., Zhai, A., Pirani, S. L., Connors, C., Péan, S., Berger, N., Caud, Y., Chen, L., Goldfarb, M. I., Gomis, M., Huang,
255   K., Leitzell, E., Lonnoy, J. B. R., Matthews, T. K., Maycock, T., Waterfield, O., Yelekçi, R. Y., and Zhou, B.: IPCC: Climate Change 2021:
256   The Physical Science Basis. Contribution of Working Group I to the Sixth Assessment Report of the Intergovernmental Panel on Climate
257   Change, Cambridge University Press, 2021.

258 Moon, S. and Ha, K.-J.: Future changes in monsoon duration and precipitation using CMIP6, npj Climate and Atmospheric Science, 3, 1–7,
259   2020.

260 O'Neill, B. C., Tebaldi, C., Van Vuuren, D. P., Eyring, V., Friedlingstein, P., Hurtt, G., Knutti, R., Kriegler, E., Lamarque, J.-F., Lowe, J.,
261   Meehl, J., Moss, R., Riahi, K., and Sanderson, B. M.: The scenario model intercomparison project (ScenarioMIP) for CMIP6, Geoscientific
262   Model Development, 9, 3461–3482, https://doi.org/10.5194/gmd-9-3461-2016, 2016.

263 O'Neill, B. C., Kriegler, E., Ebi, K. L., Kemp-Benedict, E., Riahi, K., Rothman, D. S., van Ruijven, B. J., Van Vuuren, D. P., Birkmann, J.,
264   Kok, K., Levy, M., and Solecki, W.: The roads ahead: Narratives for shared socioeconomic pathways describing world futures in the 21st
265   century, Global Environmental Change, 42, 169–180, https://doi.org/10.1016/j.gloenvcha.2015.01.004, 2017.

266 Park, J., Kim, H., Wang, S.-Y. S., Jeong, J.-H., Lim, K.-S., LaPlante, M., and Yoon, J.-H.: Intensification of the East Asian summer monsoon
267   lifecycle based on observation and CMIP6, Environmental Research Letters, 15, 0940b9, 2020.

268 Qu, X., Huang, G., and Zhou, W.: Consistent responses of East Asian summer mean rainfall to global warming in CMIP5 simulations,
269   Theoretical and applied climatology, 117, 123–131, 2014.

270 Seo, K.-H., Ok, J., Son, J.-H., and Cha, D.-H.: Assessing future changes in the East Asian summer monsoon using CMIP5 coupled models,
271   Journal of climate, 26, 7662–7675, 2013.

272 Tebaldi, C., Debeire, K., Eyring, V., Fischer, E., Fyfe, J., Friedlingstein, P., Knutti, R., Lowe, J., O'Neill, B., Sanderson, B., Van Vuuren, D.,
273   Riahi, K., Meinshausen, M., Nicholls, Z., Hurtt, G., Kriegler, E., Lamarque, J., Meehl, G., Moss, R., Bauer, S. E., Boucher, O., Brovkin,
274   V., Golaz, J., Gualdi, S., Guo, H., John, J. G., Kharin, S., Koshiro, T., Ma, L., Olivié, D., Panickal, S., Qiao, F., Rosenbloom, N., Schupfner,
275   M., Seferian, R., Song, Z., Steger, C., Sellar, A., Swart, N., Tachiiri, K., Tatebe, H., Voldoire, A., Volodin, E., Wyser, K., Xin, X., Xinyao,
276   R., Yang, S., Yu, Y., and Ziehn, T.: Climate model projections from the Scenario Model Intercomparison Project (ScenarioMIP) of CMIP6,
277   Earth System Dynamics Discussions, 2020, 1–50, https://doi.org/10.5194/esd-2020-68, 2020.

278 Van Vuuren, D. P., Kriegler, E., O'Neill, B. C., Ebi, K. L., Riahi, K., Carter, T. R., Edmonds, J., Hallegatte, S., Kram, T., Mathur, R., et al.:
279   A new scenario framework for climate change research: scenario matrix architecture, Climatic Change, 122, 373–386, 2014.

280 Volonté, A., Muetzelfeldt, M., Schiemann, R., Turner, A. G., and Klingaman, N.: Magnitude, scale, and dynamics of the 2020 mei-yu rains
281   and floods over China, Advances in Atmospheric Sciences, 38, 2082–2096, 2021.

282 Wang, B., Jin, C., and Liu, J.: Understanding future change of global monsoons projected by CMIP6 models, Journal of Climate, 33, 6471–
283   6489, 2020.

284 Wang, B. et al.: Rainy season of the Asian–Pacific summer monsoon, Journal of Climate, 15, 386–398, 2002.

285 WCRP: CMIP6 data, https://esgf-node.llnl.gov/search/cmip6/.

Earth System
Dynamics
Discussions

Open Access

EGU

286 Weedon, G., Gomes, S., Viterbo, P., Shuttleworth, W. J., Blyth, E., Oesterle, H., Adam, J., Bellouin, N., Boucher, O., and Best, M.: Creation
287   of the WATCH forcing data and its use to assess global and regional reference crop evaporation over land during the twentieth century,
288   Journal of Hydrometeorology, 12, 823–848, https://doi.org/10.1175/2011JHM1369.1, 2011.
289 Wilcox, L. J., Liu, Z., Samset, B. H., Hawkins, E., Lund, M. T., Nordling, K., Undorf, S., Bollasina, M., Ekman, A. M., Krishnan, S., et al.:
290   Accelerated increases in global and Asian summer monsoon precipitation from future aerosol reductions, Atmospheric Chemistry and
291   Physics, 20, 11955–11977, 2020.
292 Xin, X., Wu, T., Zhang, J., Yao, J., and Fang, Y.: Comparison of CMIP6 and CMIP5 simulations of precipitation in China and the East Asian
293   summer monsoon, International Journal of Climatology, 40, 6423–6440, 2020.
294 Yihui, D., Yanju, L., and Yafang, S.: East Asian summer monsoon moisture transport belt and its impact on heavy rainfalls and floods in
295   China, , 31, 629–643, 2020.
296 Yu, T., Chen, W., Gong, H., Feng, J., and Chen, S.: Comparisons between CMIP5 and CMIP6 models in simulations of the climatology and
297   interannual variability of the east asian summer Monsoon, Climate Dynamics, 60, 2183–2198, 2023.